VNU Journal of Science: Natural Sciences and Technology, Vol. 41, No. 4 (2025) 60-73

VNU Journal of Science: Natural Sciences and Technology

Journal homepage: https://js.vnu.edu.vn/NST

Original Article

Production of Biochar from Sugarcane Bagasse using a One-Stage Pyrolysis Method for Crystal Violet Adsorption in Aqueous Environment

Vo Thuy Vi[1], Tran Minh Quang[2], Bui Thi Hoa[3], Bui Xuan Vuong[*,4]

[1]*Ho Chi Minh City University of Industry and Trade, 140 Le Trong Tan, Tay Thanh, Ho Chi Minh, Vietnam*
[2]*Le Trong Tan High School, Tan Son Nhi, Ho Chi Minh, Vietnam*
[3]*Electric Power University, 235 Hoang Quoc Viet, Nghia Do, Hanoi, Vietnam*
[4]*Sai Gon University, 273 An Duong Vuong, Cho Quan, Ho Chi Minh, Vietnam*

Received 05th February 2025
Revised 21st November 2025; Accepted 04th December 2025

Abstract: Biochars were prepared by anaerobic heating of sugarcane bagasse at different temperatures of 400 °C, 500 °C, 600 °C, and 700 °C for 3 hours. The biochar samples, denoted as biochar-400 °C, biochar-500 °C, biochar-600 °C, and biochar-700 °C, were used to adsorb crystal violet dye in an aqueous medium. Physico-chemical methods such as XRD, FTIR, BET, and SEM were used to evaluate the synthesized biochar materials. The concentration of crystal violet solutions was determined using UV-Vis spectroscopy at the maximum absorption wavelength of 590 nm. The results showed that the biochar samples had good adsorption capacity for crystal violet dye, with the maximum adsorption capacity of biochar-400 °C, biochar-500 °C, biochar-600 °C, and biochar-700 °C being 154.6, 160.8, 182.8, and 168.6 mg/g, respectively. The biochar-600 °C sample has the highest adsorption capacity, consistent with its physico-chemical properties such as the highest porosity and specific surface area. Therefore, the cheap and simple prepared biochar has great potential to be used as an adsorbent material to remove crystal violet dye in an aqueous environment.

Keywords: Sugarcane bagasse; pyrolysis; adsorption, crystal violet, UV-Vis.

1. Introduction

The development of the textile industry always entails negative impacts on the aquatic environment due to the discharge of persistent organic dyes that are harmful to humans, marine animals, and plants [1]. Among organic dyes, crystal violet with the formula $C_{25}H_{30}N_3Cl$ - is a triarylmethane dye, widely used in the textile industry. It is a potent color pollutant that hinders light penetration through water, harming living organisms. Moreover, exposure to crystal violet through inhalation or direct contact is dangerous to the human body,

* Corresponding author.
E-mail address: bxvuong@sgu.edu.vn

https://doi.org/10.25073/2588-1140/vnunst.5863

causing respiratory and renal failure, skin and gastrointestinal irritation, and cytotoxicity. Crystal violet is even reported to be a carcinogen [2]. Crystal violet contamination in aquatic environments threatens human health and marine life; therefore, removing crystal violet from textile wastewater is urgent. Over the years, several methods have been used to treat crystal violet in sewage, including electrocoagulation, membrane separation, electrochemical oxidation, and micellar catalysis [3]. However, the high cost and requirement for technological equipment have limited the use of the above methods. Therefore, using environmentally friendly and low-cost adsorbents to remove dyes from wastewater has attracted the attention of scientists. Biochar is a carbon-rich material produced by the pyrolysis of biomass in a closed system with little or no oxygen, which presents the potential to be used as a low-cost adsorbent to remove crystal violet colorants polluting the water environment [4]. Although its adsorption efficiency is not as high as that of activated carbon, biochar is much cheaper because it is made from a variety of biomass sources, such as sewage sludge, livestock and poultry manure, organic solid waste, rice husks, oak bark, pine wood, coffee grounds, and sugarcane bagasse [5]. Several scientific publications have reported on the use of biochar made from agricultural biomass sources to remove crystal violet from textile wastewater. Two biochars derived from Melia azedarach seed were prepared through a single-stage thermal decomposition of the feedstock under O_2-deficient conditions at 700 ^oC (designated B-700) and hydrothermal carbonization followed by pyrolysis at 700 ^oC (designated HB-700) [6]. Biochar samples were used to adsorb crystal violet in aqueous media under different experimental conditions, such as pH, contact time, adsorbent content, and temperature. The results showed that the biochar samples have good adsorption capacity for crystal violet dye in aqueous media, with maximum adsorption capacities of 119.4 $mg.g^{-1}$ for sample B-700 and 209 $mg.g^{-1}$ for sample HB-700, respectively. Rice husk, an agricultural by-product, was calcined at temperatures ranging from 100 ^oC to 700 ^oC to prepare biochar [7]. Synthetic biochar samples were used to adsorb crystal violet from the aqueous medium. The study showed that the adsorption of crystal violet by biochar is consistent with the Langmuir adsorption isotherm model; additionally, the adsorption capacity of biochar for the removal of crystal violet is 25.46 mg/g. Biochar was made from rice husk and then modified with xanthate to enhance the adsorption capacity of crystal violet in an aqueous medium [8]. Experiments showed that the adsorption capacity of modified biochar was significantly increased compared to the unmodified biochar sample, with adsorption capacities of 90.02 mg/g and 62.85 mg/g for modified and unmodified biochar materials, respectively.

Many other studies have also focused on the preparation of biochar for dye removal from agricultural biomass sources such as peanut shells [9], straw [10], walnut shells [11], date palm kernels [12], and cashew nut shells [13]. In this study, we prepared biochar from sugarcane bagasse using a one-stage pyrolysis method and then used the biochar samples to adsorb crystal violet in the aqueous medium. Different parameters of the adsorption experiment, such as pH, adsorption time, adsorbent mass, and initial concentration of crystal violet, were investigated. We also evaluated the mechanism of crystal violet adsorption by biochar based on the Langmuir and the Freundlich isotherm adsorption models.

2. Experimental

2.1. Process of Making Biochar from Bagasse

Bagasse collected from the Can Tho Sugarcane Joint Stock Company was washed thoroughly to remove impurities. The clean bagasse was boiled with distilled water for 30 minutes to remove all-natural sugar and then dried at 80 °C in a drying oven for 24 hours to obtain raw bagasse. The raw bagasse was then

heated anaerobically in a tightly covered crucible at different temperatures, 400 °C, 500 °C, 600 °C, and 700 °C, for 3 hours. In this study, temperatures lower than 300 °C did not burn all the bagasse to form biochar, so the temperature chosen to produce biochar was 400 °C or higher. At the end of the calcination process, the obtained biochar was ground with a mortar and then sieved through a 150-350 µm sieve. The sieved samples were tightly packed into jars with lids and stored for use in subsequent experiments. The biochar samples were labeled according to the manufacturing temperatures at 400 °C, 500 °C, 600 °C, and 700 °C; as biochar-400 °C, biochar-500 °C, biochar-600 °C, and biochar-700 °C, respectively. The schematic diagram of the manufacturing process and biochar products is presented in Figure 1.

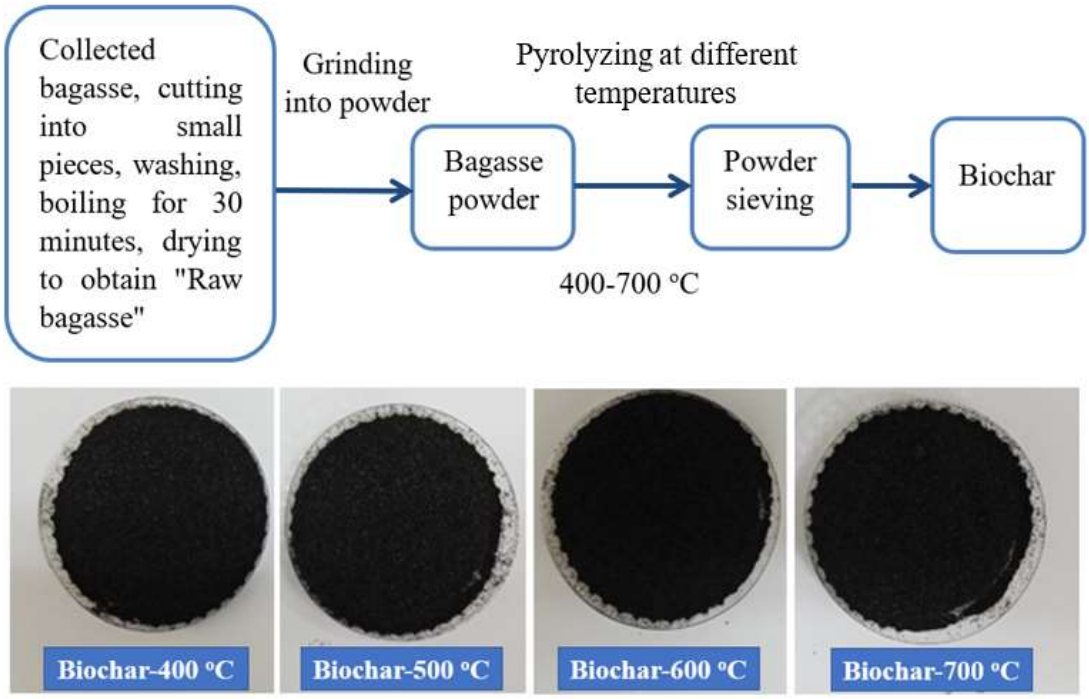

Figure 1. Schematic diagram of biochar production from sugarcane bagasse and photos of the obtained biochar samples.

2.2. Adsorption Experiment of Crystal Violet using Biochar

2.2.1. Establishing the Adsorption Standard Curve Equation

The maximum adsorption wavelength of crystal violet solution is 590 nm, determined by measuring the UV-Vis spectrum of crystal violet solution at a concentration of 6 mg/L in the wavelength range of 300-700 nm. Based on this wavelength, a calibration curve was constructed, presenting the relationship between the CV concentrations from 1 mg/L to 10 mg/L and their maximum absorbance value (Abs), as shown in Figure 2.

2.2.2. Adsorption Experiment

The biochar samples were placed in Erlenmeyer flasks (250 mL capacity) containing 100 mL of crystal violet solution. The reaction flasks were sealed with ground glass stoppers and were placed in a thermostatic shaking system (GFL 1083). At the end of the reaction, centrifugation was performed to separate the biochar fraction, and the filtered solution was used to measure the remaining crystal violet concentration using a UV-Vis spectrophotometer. The adsorption efficiency R (%) is calculated according to the formula:

$$R = \frac{C_o - C}{C_o}. 100\% \quad (1)$$

In which, C_o - initial concentration (mg/L); C - remaining concentration after adsorption; R - removal (%).

Experimental parameters, such as pH, reaction time, adsorbent content, and crystal violet solution concentration, were investigated to evaluate the adsorption capacity of biochar.

2.2.2.1. Effect of pH

To evaluate the effect of pH on the adsorption capacity of biochar material, experiments were carried out with crystal violet solutions at different pH values from 2 to 11 using 0.1M NaOH and 0.1M HCl solutions for adjustment. The remaining parameters, such as adsorbent mass, reaction time, crystal violet concentration, and stirring speed, were 0.02 g, 10 min, 30 mg/L, and 100 rpm, respectively.

2.2.2.2. Effect of Adsorption Time

Experiments on the effect of adsorption time were carried out by changing the adsorption time to 0, 3, 5, 8, 10, 15, 20, 25, 30, 35, 40, 45, and 50 minutes. The remaining parameters, such as adsorbent mass, crystal violet concentration, and stirring speed, were 0.02 g, 30 mg/L, and 100 rpm, respectively.

2.2.2.3. Effect of Biochar Content

Experiments on the effect of adsorbent content were carried out by varying the amount of biochar used to 0.00, 0.01, 0.02, 0.03, 0.04, and 0.05 g. The remaining parameters, such as crystal violet concentration, stirring speed, and reaction time, were 30 mg/L, 100 rpm, and 10 minutes, respectively.

2.2.2.4. Effect of Crystal Violet Solution Concentration

Experiments on the effect of crystal violet concentration on the adsorption process of biochar were carried out by changing the initial crystal violet concentration to 10, 30, 50, 70, 100, and 150 mg/L. The remaining parameters, such as the mass of biochar, stirring speed, and reaction time, were 0.02 g, 100 rpm, and 10 minutes, respectively.

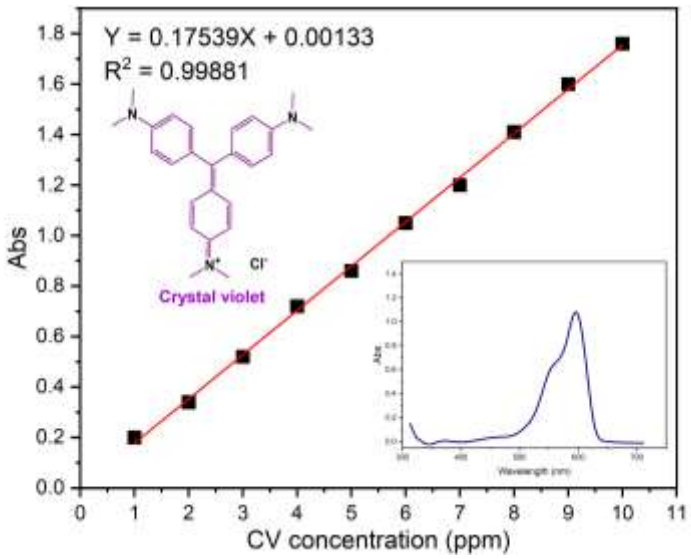

Figure 2. Calibration curve of crystal violet solutions at 590 nm.

2.2.3. Adsorption Isotherm Equation

Experiments were performed using biochar to adsorb crystal violet at different concentrations, as presented above. The experimental data were calculated and verified for their fits to the Langmuir and Freundlich isotherm adsorption models, as shown in equations (1) and (2).

Langmuir isotherm model:

$$\frac{C_e}{Q_e} = \frac{C_e}{Q_m} + \frac{1}{K_L.Q_m} \quad (2)$$

Freundlich isotherm model:

$$LnQ_e = LnK_F + \frac{1}{n}.LnC_e \quad (3)$$

The Q_e value is calculated as:

$$Q_e = \frac{(C_o - C_e).V}{m} \quad (4)$$

Here, C_e (mg/L) and Q_e (mg/g) represent the concentration and adsorption capacity at equilibrium, respectively; Q_m (mg/g) is the maximum adsorption capacity; K_L and K_F are the Langmuir and Freundlich constants, respectively; n is the Freundlich coefficient.

2.3. Methods of Physical-Chemical Analysis

The structure and phase composition of the materials were analyzed using X-ray powder diffraction (XRD). The samples were finely ground and analyzed on a PANalytical Empyrean diffractometer with a Cu-Kα wavelength (λ = 1.5406 Å) at a step size of 0.026°. Fourier Transform Infrared Spectroscopy (FTIR) was used to determine the functional groups present in the synthesized materials. The analysis was performed on a Thermo Scientific Nicolet 6700 spectrometer in the infrared range of 400 – 4000 cm^{-1} with a resolution of 2 cm^{-1}. BET (Brunauer – Emmett – Teller) method was used to determine the values of specific surface area, pore volume, and average pore diameter in synthesized materials based on nitrogen adsorption/desorption. The surface structure morphology of the synthesized biochar samples was observed using a scanning electron microscope. The concentration of the crystal violet solution was determined using a UV-Vis spectrophotometer based on the standard curve equation determined above.

3. Results and Discussion

3.1. Physical-chemical Characteristics of Synthesized Biochars

3.1.1. XRD and FTIR Analysis

Figure 3a shows the XRD patterns of biochar samples prepared from sugarcane bagasse at different temperatures. All four XRD spectra show broad diffraction patterns from 10 – 70° (2θ), confirming the amorphous structure of the prepared biochar materials. This result is similar to other previously published studies [14, 15]. Amorphous materials exhibit disordered structures, leading to poor interference of X-rays on the sample surface, so they do not produce sharp peaks but often broad peaks or diffraction halos. The structural characteristics of sugarcane bagasse or wood are that they contain organic compounds such as cellulose, hemicellulose, and lignin; they have a crystalline polymer structure arranged periodically by many multi-sided organic frameworks (5, 6 sides) with the framework vertices being C elements When bagasse is anaerobically heated, part of the C elements are burned to release CO_2 gas, causing the crystalline polymer structure to deform, losing its periodic structure, creating an amorphous state of the material. On the other hand, the burning of C elements leaves holes in the structure of biochar materials, making them porous and having a large specific surface area, making them suitable as an adsorbent for toxic gases or dyes in polluted water environments. When considering each synthesis temperature, the XRD spectrum of the biochar sample at 400 °C shows the most amorphous structure due to the widest and lowest diffraction halo; the XRD spectrum of the biochar samples at higher temperatures shows that the shape of the diffraction halo tends to narrow at the center around 22° (2θ), which is characteristic of the formation of the SiO_2 phase with a semi-crystalline structure. Thus, when the synthesis temperature increases, the biochar material tends to crystallize; this observation is clearly shown in the biochar sample prepared at 700 °C, where the XRD spectrum shows 02 peaks at around 22° and 29° (2θ). Normally, when the material changes from the amorphous state to the crystalline state, the porous structure characteristic of the material is reduced because the atoms in the material structure tend to be arranged more tightly.

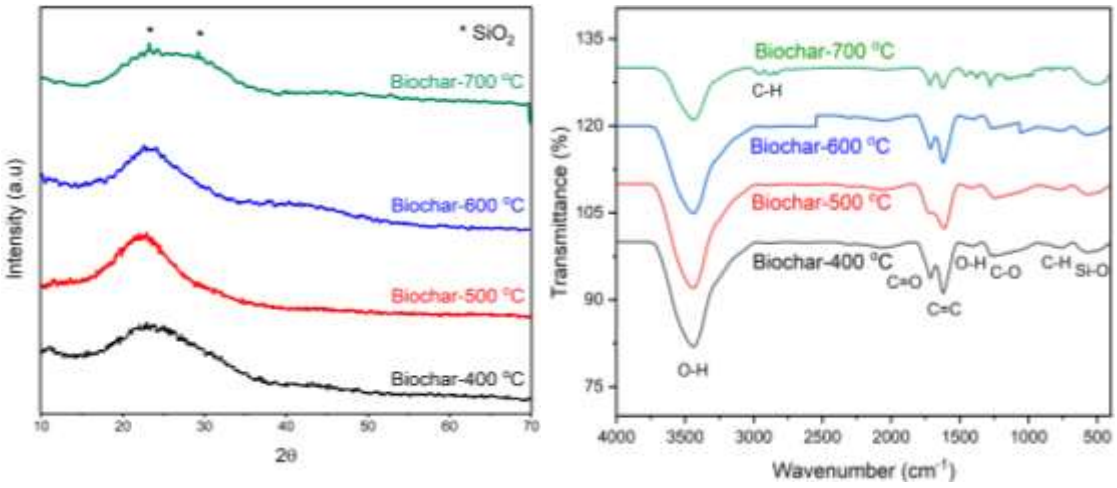

(3a) (3b)

Figure 3. XRD diagrams and FTIR spectra of biochar prepared at different temperatures.

Figure 3b shows the FTIR spectra of biochar samples prepared at different temperatures. It was observed that all four FTIR spectra showed the functional groups of biochar [16, 17]. A broad IR absorption band at 3454 cm^{-1} corresponding to the stretching vibration of -OH groups was observed in all biochar samples, demonstrating the presence of hydroxyl groups on the biochar surface. Double IR absorption bands, at about 2981 cm^{-1} and 2854 cm^{-1}, were assigned to the stretching vibration of the C-H bond in the functional groups $-CH_2$ and $-CH_3$. The two absorption bands at 1721 and 1631 cm^{-1} corresponded to the stretching vibration of the C=O bond and the C=C bond; the absorption band at 1410 cm^{-1} was characteristic of the O-H bond; the oscillation at 1234 cm^{-1} was characteristic of the C-O group; the oscillation at about 783 cm^{-1} was characteristic of the bending vibration of the plane of the cyclic C-H bond. In addition, the FTIR spectrum also showed an oscillation at about 572 cm^{-1}, which was characteristic of the stretching vibration of the Si-O bond. When the temperature of biochar preparation increased, the functional groups showed a shift, decreasing in intensity; this demonstrates the influence of fabrication temperature on the structure of functional groups in biochar.

3.1.2. Porous Structure and Surface Morphology

The porous structure properties of the biochar materials were evaluated using the Brunauer–Emmett–Teller (BET) method. The biochar samples were degassed to remove moisture in the pores and then subjected to N_2 adsorption/desorption. The adsorption cross-section of the adsorbed N_2 molecules was taken as 0.162 nm^2 to calculate the specific surface area according to ISO 9277. The pore volume (V_p) was obtained from the amount of N_2 adsorbed by the sample in the relative pressure range ($0.9947 < P/P_o < 0.9956$). The formula $d = V_p/S_{BET}$ determined the average pore diameter. Figure 4a shows the adsorption/desorption isotherms of biochar samples. The shape of the isotherms shows that the synthesized biochar materials belong to type IV according to the IUPAC classification. According to IUPAC, these are materials with a mesoporous structure with an average pore diameter from 2 to 50 nm [17]. Also, according to IUPAC, the H_1-type adsorption/desorption hysteresis loops are characteristic of many pores in the mesoporous structure of biochar materials. Comparing the shape of the adsorption isotherm shows that the N_2 adsorption/desorption capacity increases

gradually when the prepared temperature rises from 400 °C to 500 °C, reaches a maximum at 600 °C, and then decreases at 700 °C. This explains that the ability to burn organic compounds in bagasse increases when the temperature rises, creating more pores for the biochar material. However, when the temperature is higher than 700 °C, the material tends to sinter to crystallize together into denser forms, leading to a decrease in adsorption capacity. This observation is consistent with the above XRD analysis, as the XRD diagram of the biochar sample at 700 °C shows a clear crystalline phase of SiO_2.

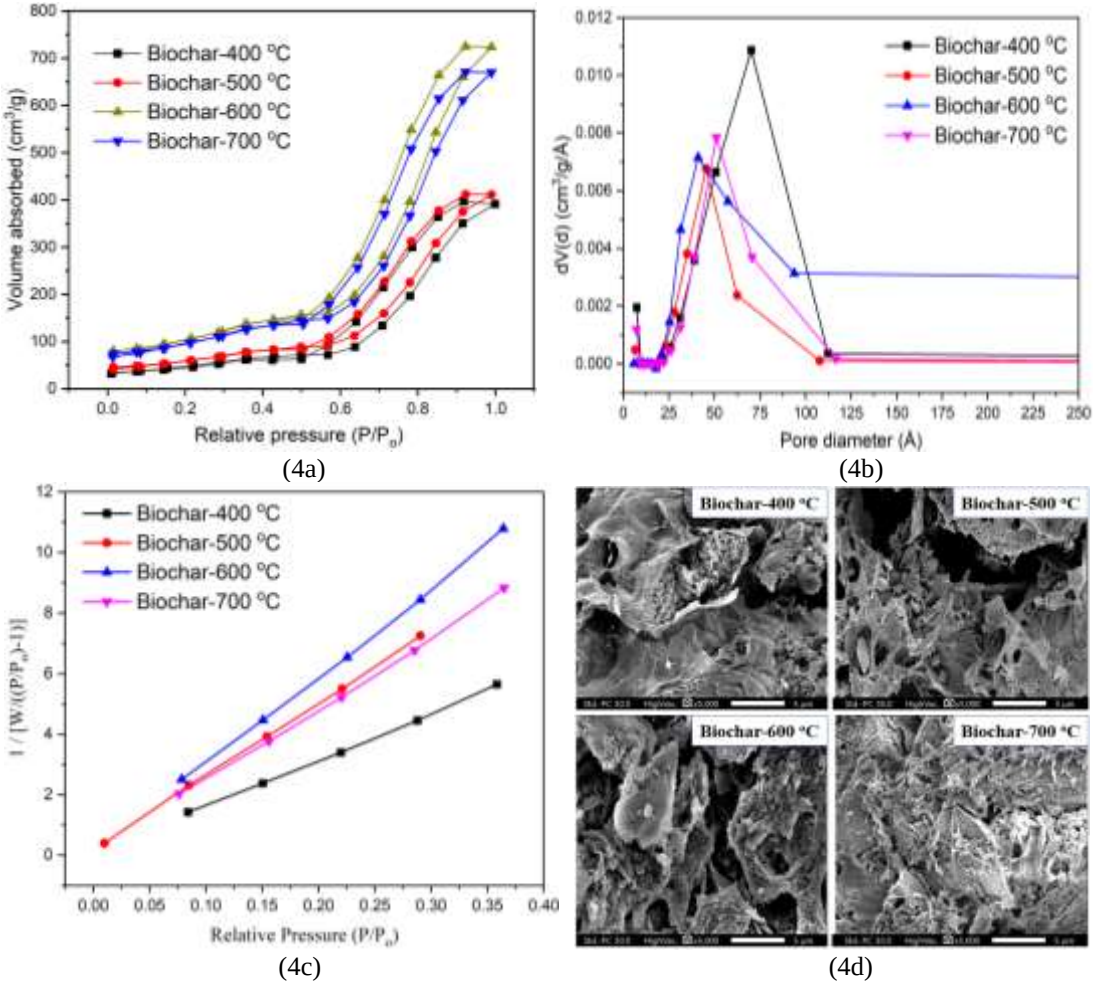

Figure 4. BET and SEM analysis of biochar materials.

The pore size distribution of the synthesized biochar samples is shown in Figure 4b. The pore size varied from 20 to 115 Å (2-11.5 nm) for all the synthesized samples. The average pore diameter of the biochar sample prepared at 400 °C was the largest, about 70 Å; then it gradually decreased in the sample prepared at 500 °C (45.4 Å) and 600 °C (41 Å); then it increased again in the biochar sample prepared at 700 °C (51 Å). The multi-point BET analysis is shown in Figure 4c. The structural data on pore volume, average pore diameter, and specific surface area are presented in Table 1. All four biochar samples synthesized in this study have similar or higher specific surface area values than samples produced from other

biomass sources, demonstrating the adsorption potential of biochar prepared from sugarcane bagasse in this study [6, 14, 15]. It can be seen that the pore volume and specific surface area of the biochar sample increased from 400 °C to 600 °C, then decreased at 700 °C. The data showed that the biochar sample prepared at 600 °C gave the best porous structure (V_{pore} = 1.376 cm^3/g; specific surface area S_{BET} = 388.2 m^2/g). This result is consistent with the XRD analysis above; when the temperature increases, it enhances the burning of C sites to create pores for the material, but when the temperature is too high, it will lead to sintering to form a crystalline-agglomerated state of the material, causing the porosity to decrease.

Table 1. Structural data of biochar materials

Sample	Pore volume (cm^3/g)	Average pore diameter (nm)	Specific surface area (m^2/g)
Biochar-400 °C	0.791	7.00	181.3
Biochar-500 °C	0.881	4.54	220.5
Biochar-600 °C	1.376	4.10	388.2
Biochar-700 °C	1.273	5.10	359.4
Pyrolysis Biochar from Melia azedarach [6]	0.225	3.41	405.1
Hydrothermal Biochar from Melia azedarach [6]	0.223	3.42	389.74
Biochar from rice husk [14]	49.6	22.4	267.90
Biochar from bamboo [15]	0.277	-	369.59
Biochar from Oak wood [15]	-	53.11	231.15

Figure 4c shows SEM images of biochar samples prepared at different temperatures. The biochar sample prepared at 400 °C shows a 3D structure with a rough surface and wide gaps, creating a porous material structure. Observation also shows large ring-shaped patches, possibly made by undecomposed organic structures. The biochar sample at 500 °C still has ring-shaped membranes but is more fragmented because the material was heated at a higher temperature; the material's surface has many large and small pores that are interconnected to create a porous structure. When the biochar was prepared at higher temperatures of 600 °C, more organic matter particles were burned, creating small, rough grain structures that generate smaller pores on the surface next to the large pores. The presence of micropores, in addition to the usual macropores, gives a high value to the specific surface area of the material. This observation is consistent with the BET analysis results above, where the biochar sample at 600 °C has the largest specific surface area. When the biochar sample was prepared at 700 °C, the material surface still showed a rough, porous state, but the macropores seemed to decrease; this is explained by the phenomenon of sintering at high temperatures, in which small-sized particles tend to gather to form larger aggregates, making the material denser. The observation of SEM images of the biochar samples in this study is similar to previous studies [14, 15], where the biochar samples showed a porous 3D surface structure with potential for application as an adsorbent material.

3.2. Evaluation of Crystal Violet Adsorption Capacity using Biochar

3.2.1. pH Point Zero Charge and Effect of pH

The pH point zero charges (pH_{pzc}) of the biochar materials were determined using the

pH-drift (pH-shifting) method [18]. A series of 50 mL NaCl solutions (0.01 M) was prepared with initial pH (pH_i) values ranging from 2.0 to 11.0, adjusted using HCl or NaOH solutions. To each solution, 30 g of biochar powder was added, followed by sealing and shaking at 200 rpm for 6 hours at room temperature. After this period, the value of the final pH (pH_f) of each sample was recorded. The pH change ($\Delta pH = pH_f - pH_i$) was calculated, and the pH_{pzc} was identified as the point at which $\Delta pH = 0$. In this study, the pH point zero charges were 6.9, 7.6, 7.4, and 7.2 for biochar-400 ^oC, biochar-500 ^oC, biochar-600 ^oC, and biochar-700 ^oC, respectively. Figure 5a shows the effect of pH on the biochar samples' crystal violet adsorption efficiency. The initial pH of the aqueous medium affects the surface area and dissociation of the functional groups of the adsorbent, as well as the degree of ionization of the adsorbent, thus significantly impacting the removal of crystal violet dye. It was observed that the adsorption of crystal violet dye was enhanced as the pH increased from 2 to 7, after which the adsorption percentage did not change much until the pH was 11. This result is explained by the fact that in an acidic environment, the high concentration of H^+ ions will compete with the CV dye cations on the available active sites. As the pH value continues to increase, the active sites will be more ionized, which is suitable for effective interaction with crystal violet dye to enhance the adsorption efficiency [21, 22]. Thus, the adsorption of crystal violet dye by biochar is suitable in neutral or basic environments with $pH > pH_{pzc}$ because the biochar surface carries a negative charge and is suitable for the adsorption of cationic crystal violet dye.

3.2.2. Effect of Reaction Time

Figure 5b shows the results of the crystal violet solution adsorption capacity survey over the reaction time of biochar samples prepared at different temperatures. The adsorption rate of crystal violet increased rapidly in the first 10 minutes and reached adsorption equilibrium. The quick adsorption of crystal violet is due to the porous structure with the large specific surface area of biochar samples, creating many surface-active sites of the adsorbent for effective adsorption of crystal violet dye. After the equilibrium adsorption time of 10 minutes, the percentage of absorbed crystal violet remained almost unchanged because the active centers of the biochar adsorbent were wholly occupied. Thus, the biochar samples' crystal violet adsorption rate was relatively fast to achieve adsorption equilibrium, similar to the biochar material prepared in the previous study [15]. Among four biochar samples, the biochar-600 ^oC gave the highest adsorption efficiency at equilibrium, reaching 97.2%, followed by the biochar-700 ^oC (94.1%), the biochar-500 ^oC (84.3%), and the biochar-400 ^oC (83.5%). This result is consistent with the corresponding porous structure characteristics of the biochar samples; the more significant the porous structure of the material, the higher the crystal violet adsorption capacity and vice versa.

3.2.3. Effect of Biochar Content

Figure 5c shows the effect of biochar adsorbent dosage on the adsorption efficiency of crystal violet dye under the studied conditions. The adsorption ratio of the dye increased with increasing adsorbent dosage in the range of 0.01-0.02 g at a fixed dye concentration. Further, with an increase in adsorbent dosage from 0.01 g to 0.02 g, the surface area was increased, and the number of active sites increased, improving the adsorption efficiency [15, 16]. When the adsorbent dosage increased from 0.03 g to 0.05 g, the adsorption percentage of the dye remained almost constant or increased very slowly. This may be because when the adsorbent dosage increased, the adsorbent particles would be compressed together, and no active sites would be available for further adsorption of crystal violet dye [15, 16].

3.2.4. Effect of Crystal Violet Solution Concentration

Figure 5d shows the results of the investigation of the effect of the initial concentration of crystal violet dye on the adsorption efficiency of the prepared biochar at different temperatures. The results showed that

as the initial concentration of crystal violet dye increased, the adsorption capacity of the biochar samples decreased. The biochar adsorbent has enough active sites at low dye concentrations. After all, the vacant active sites on the adsorbent surface are filled with crystal violet dye [15]. Saturation of the adsorbent surface may occur as the concentration of the dye increases. Saturation occurs due to the limited surface area of the adsorbent, leading to a decrease in the removal efficiency of the dye in the aqueous medium.

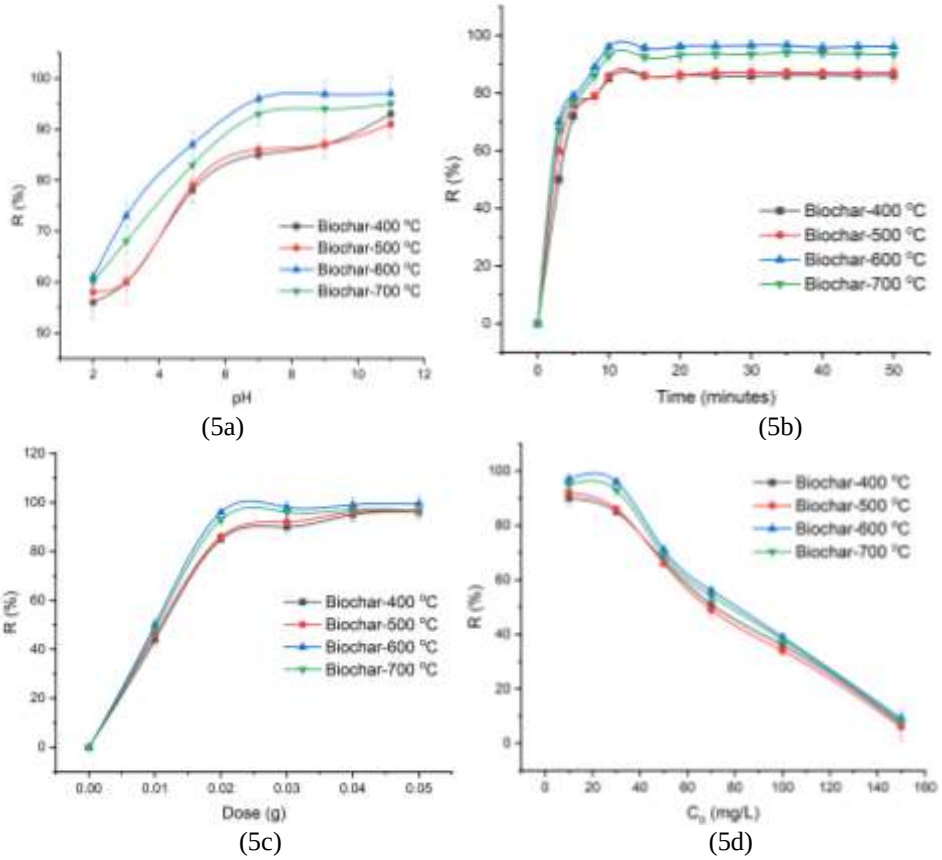

Figure 5. Experiment factors affecting the adsorption capacity of crystal violet in solution by biochars.

3.3. Isothermal Adsorption Mechanism

To determine the adsorption isotherm equations, experiments using biochar to adsorb crystal violet solution at different concentrations were performed. Table 2 presents the experimental and calculated data. From the calculated values, the Langmuir and Freundlich adsorption isotherms were constructed using Origin software.

Table 2**.** Calculated data for building Langmuir and Freundlich isotherm models

Biochar-400 °C	C_o	10	30	50	70	100	150
	C_e	1	4.5	16.5	34.3	64	120
	C_e/Q_e	0.22222	0.03529	0.0985	0.1922	0.3556	0.8
	LnC_e	0	1.5041	2.8034	3.5352	4.1589	4.7875
	LnQ_e	3.8067	4.8481	5.1210	5.1846	5.1930	5.0106

Biochar-500 °C	C_e	0.8	4.2	17	35.7	66	118.5
	C_e/Q_e	0.0174	0.0326	0.1030	0.2082	0.3882	0.7524
	LnC_e	-0.2231	1.4350	2.8332	3.5751	4.1896	4.7749
	LnQ_e	3.8286	4.8598	5.1060	5.1446	5.1358	5.0594
Biochar-600 °C	C_e	0.3	1.2	14.5	30.8	61	114
	C_e/Q_e	0.0062	0.0083	0.0817	0.1571	0.3128	0.6333
	LnC_e	-1.2039	0.1823	2.6741	3.4275	4.1108	4.736
	LnQ_e	3.8815	4.9698	5.1789	5.278	5.273	5.1929
Biochar-700 °C	C_e	0.5	2.1	15.5	32.2	62	117
	C_e/Q_e	0.0105	0.0151	0.0899	0.1704	0.3263	0.7091
	LnC_e	-0.693	0.7419	2.7408	3.4719	4.1271	4.7621
	LnQ_e	3.8607	4.9380	5.1504	5.2417	5.2470	5.1059

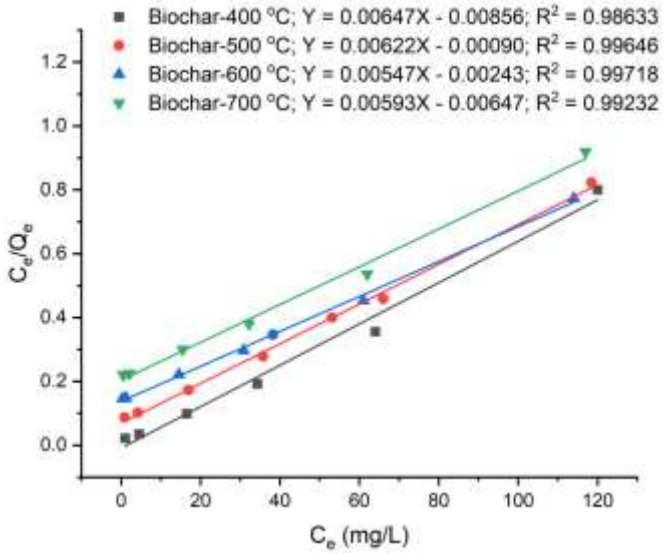

Figure 6. Langmuir isotherm adsorption model
of biochar samples prepared at different temperatures

Table 3. Maximum adsorption capacity data of biochar materials

Sample	Q_m (mg/g)	References
Biochar-400 °C	154.6	Current study
Biochar-500 °C	160.8	Current study
Biochar-600 °C	182.8	Current study
Biochar-700 °C	168.6	Current study
Pyrolysis Biochar from Melia Azedarach	19.8	[6]
Hydrothermal Biochar from Melia Azedarach	19.9	[6]
Biochar from Sugarcane Bagasse	82.96	[18]
Biochar from Palm Kernel Fiber	78.9	[19]
Biochar from Pineapple Leaf Powder	78.22	[20]

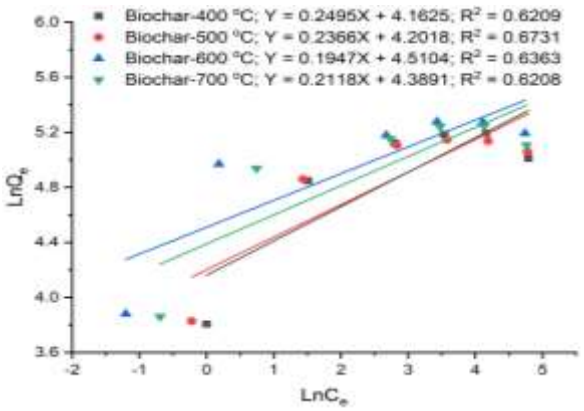

Figure 7. Freundlich isotherm adsorption model of biochar samples prepared at different temperatures.

Figure 6 shows the Langmuir isotherm adsorption models of biochar samples. All biochar samples fit the Langmuir isotherm adsorption model well because of their high correlation coefficient R^2 values, close to 1. The corresponding R^2 values for the biochar-400 °C (0.98633), biochar-500 °C (0.99646), biochar-600 °C (0.99718), and biochar-700 °C (0.99232). The high R^2 values indicate that crystal violet adsorption occurs on biochar materials at active sites as a monolayer [17]. The linear equations Y = AX + B according to the Langmuir isotherm adsorption model for the biochar samples are biochar-400 °C (Y = 0.00647X – 0.00856); biochar-500 °C (Y = 0.00622X – 0.000903); biochar-600 °C (Y = 0.00547X – 0.00243); biochar-700 °C (Y = 0.00593X – 0.00647). From the above-obtained equations, the maximum adsorption capacity value Q_m (mg/g) of the biochar samples can be obtained according to the formula $1/Q_m = A$ (A is the coefficient in the equation Y = AX + B) (Table 3). The maximum adsorption capacity of the biochar samples in this study was relatively high compared to biochar samples reported in previous studies [6, 18-20]. The biochar-600 °C has the highest adsorption capacity, and the lowest is biochar-400 °C. Figure 7 shows the Freundlich isotherm adsorption models of biochar samples prepared at different temperatures. The experimental points of crystal violet adsorption are observed to be scattered far from the linear line for all four models. The values of correlation coefficients R^2 are biochar-400 °C (0.62089), biochar-500 °C (0.6731), biochar-600 °C (0.63634), and biochar-700 °C (0.62075). The low R^2 values (< 0.7) indicated that the crystal violet adsorption behavior of the biochar samples did not fit the Freundlich isotherm adsorption model [14, 16].

3.4. Reusability of Biochar after CV Adsorption

Reusability is an important factor in evaluating the overall efficiency of CV adsorption by biochar. For reuse, the biochar-600 °C sample was selected to desorb CV from the solid by soaking in HCl acid solution [18]. The complete desorption of CV from the adsorbent solid was checked by UV-Vis spectroscopy. The desorbed biochar sample was then dried at 100 °C and reused for CV removal. The reusability of biochar was performed for six experimental cycles. For each experiment, 0.02 g of adsorbent was stirred with 300 mL of CV solution for 10 min at a stirring speed of 100 rpm. Figure 8 shows the adsorption performance of biochar at different reuse cycles. After six adsorption cycles, the CV removal efficiency decreased from 96.5% to 35%. Among them, the adsorption efficiency of the first four cycles was above 50%, confirming the good reuse performance of biochar [18, 19].

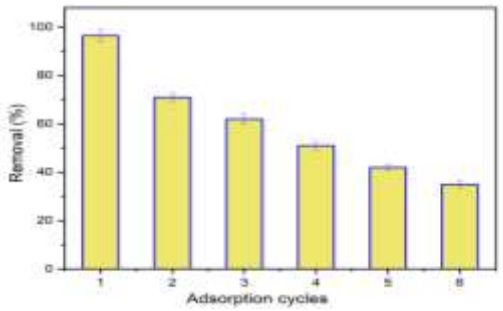

Figure 8. CV removal efficiency of biochar-600 °C after adsorption cycles.

4. Conclusion

Biochar materials were successfully synthesized by a simple one-stage pyrolysis of sugarcane bagasse in anaerobic conditions at different temperatures. Physico-chemical characteristics show that the biochar samples are amorphous materials with mesoporous structures and present functional groups. The biochar materials have relatively high specific surface areas, in which the biochar-600 °C sample has the most porous structure with pore volume V_{pore} = 1.376 (cm^3/g) and specific surface area S_{BET} = 388.2 (m^2/g). Experiments were carried out to evaluate the crystal violet adsorption capacity in the solution environment of biochars. Factors affecting the adsorption capacity were selected for investigation, such as reaction time, initial concentration of crystal violet solution, pH, and adsorbent dosage. The results of the adsorption capacity evaluation showed that all biochar samples could remove the CV crystal violet dye well; the biochar-600 °C sample showed the highest crystal violet adsorption capacity with a maximum adsorption capacity of 182.8 (mg/g). The adsorption kinetics were fitted to the Langmuir and the Freundlich isotherm adsorption models. The results showed that the biochar samples were suitable for the Langmuir isotherm adsorption model because the correlation coefficient R^2 was high, close to 1, which means that crystal violet adsorption onto the biochar surface is monolayer-based on the active sites on the material surface. In conclusion, biochars from abundant sugarcane bagasse are a cheap adsorbent material that can potentially treat crystal violet dye in an aqueous environment. Further studies are directed towards testing with real water samples or water samples containing competing ions to evaluate and exploit the effectiveness of the cheap biochar adsorbent prepared from sugarcane bagasse.

References

[1] S. Velusamy, A. Roy, S. Sundaram, T. K. Mallick, A Review on Heavy Metal Ions and Containing Dyes Removal Through Graphene Oxide-Based Adsorption Strategies for Textile Wastewater Treatment, The Chemical Record, Vol. 21, 2021, pp. 1-42, https://doi.org/10.1002/tcr.202000153.

[2] M. K. Mbacké, C. Kane, N. O. Diallo, C. M. Diop, F. Chauvet, M. Comtat, T. Tzedakis, Electrocoagulation Process Applied on Pollutants Treatment-experimental Optimization and Fundamental Investigation of the Crystal Violet Dye Removal, Journal Environment Chemical Engineering, Vol. 4, 2016, pp. 4001-4011, https://doi.org/10.1016/j.jece.2016.09.002.

[3] A. K. Mostafazadeh, A. T. Benguit, A. Carabin, P. Drogui, E. Brien, Development of Combined Membrane Filtration, Electrochemical Technologies, and Adsorption Processes for Treatment and Reuse of Laundry Wastewater and Removal of Nonylphenol Ethoxylates as Surfactants, Journal of Water Process Engineering, Vol. 28, 2019, pp. 277-292, https://doi.org/10.1016/j.jwpe.2019.02.014.

[4] K. N. A. Putri, A. Keereerak, W. Chinpa, Novel cellulose-based Biosorbent from Lemongrass Leaf Combined with Cellulose Acetate for Adsorption of Crystal Violet, International Journal of Biological Macromolecules, Vol. 156, 2020, pp. 762-772, https://doi.org/10.1016/j.ijbiomac.2020.04.100.

[5] Z. Liu, G. Han, Production of Solid Fuel Biochar from Waste Biomass by Low Temperature Pyrolysis, Fuel, Vol. 158, 2015, pp. 159-165, https://doi.org/10.1016/j.fuel.2015.05.032.

[6] A. Nouioua, D. B. Salem, A. Ouakouak, N. Rouahna, O. Baigenzhenov, A. H. Bandegharaei, Production of Biochar from Melia Azedarach Seeds for the Crystal Violet Dye Removal from Water: Combining of Hydrothermal Carbonization and Pyrolysis, Bioengineered, Vol. 14, 2023, pp. 290-306, https://doi.org/10.1080/21655979.2023.2236843.

[7] J. O. Quansah, T. Hlaing, F. N. Lyonga, P. P. Kyi, S. H. Hong, C. G. Lee, S. J. Park, Nascent Rice Husk as an Adsorbent for Removing Cationic Dyes from Textile Wastewater, Applied Science, Vol. 10, 2020, pp. 3437, https://doi.org/10.3390/app10103437.

[8] P. L. Homagai, R. Poudel, S. Poudel, A. Bhattarai, Adsorption and Removal of Crystal Violet Dye from Aqueous Solution by Modified Rice Husk, Heliyon, Vol. 8, 2021, pp. e09261, https://doi.org/10.1016/j.heliyon.2022.e09261.

[9] J. Song, W. Zou, Y. Bian, F. Su, R. Han, Adsorption Characteristics of Methylene Blue by Peanut Husk in Batch and Column Modes, Desalination, Vol. 265, 2011, pp. 119-125, https://doi.org/10.1016/j.desal.2010.07.041.

[10] Z. Wang, P. Han, Y. Jiao, D. Ma, C. Dou, R. Han, Adsorption of Congo Red using Ethylenediamine-modified Wheat Straw, Desalination and Water Treatment, Vol. 30, 2011, pp. 195-206, https://doi.org/10.5004/dwt.2011.1984.

[11] H. Aydin, G. Baysal, Y. Bulut, Utilization of Walnut Shells (Juglans Regia) as an Adsorbent for the Removal of Acid Dyes, Desalination and Water Treatment, Vol. 2, 2009, pp. 141-150, https://doi.org/10.5004/dwt.2009.251.

[12] K. Foo, B. Hameed, Preparation of Activated Carbon from Date Stones by Microwave-induced Chemical Activation: Application for Methylene Blue Adsorption, Chemical Engineering Journal, Vol. 170, 2011, pp. 338-341, https://doi.org/10.1016/j.cej.2011.02.068.

[13] P. S. Kumar, S. Ramalingam, C. Senthamarai, M. Niranjanaa, P. Vijayalakshmi, S. Sivanesan, Adsorption of Dye from Aqueous Solution by Cashew Nut Shell: Studies on Equilibrium Isotherm, Kinetics and Thermodynamics of Interactions, Desalination, Vol. 261, 2010, pp. 52-60, https://doi.org/10.1016/j.desal.2010.05.032.

[14] S. T. R. Agassin, J. Dognini, A. Paulino, Raw Rice Husk Biochar as a Potential Valuable Industrial Byproduct for the Removal of Rhodamine B from Water, Water, Vol. 15, 2023, pp. 3849, https://doi.org/10.3390/w15213849.

[15] L. Leng, Q. Xiong, L. Yang, H. Li, Y. Zhou, W. Zhang, S. Jiang, H. Li, H. Huang, An Overview on Engineering the Surface Area and Porosity of Biochar, Science of Total Environment, Vol. 763, 2021, pp. 144204, https://doi.org/10.1016/j.scitotenv.2020.144204.

[16] Y. Kuang, X. Zhang, S. Zhou, Adsorption of Methylene Blue in Water onto Activated Carbon by Surfactant Modification, Water, Vol. 2, 2020, pp. 587-601, https://doi.org/10.3390/w12020587.

[17] M. Naderi, Surface Area: Brunauer–Emmett–Teller (BET), Progress in Filtration and Separation, Vol. 14, 2015, pp. 585-608, https://doi.org/10.1016/B978-0-12-384746-1.00014-8.

[18] A. Nouioua, D. B. Salem, A. Ouakouak, N. Rouahna, O. Baigenzhenov, A. H. Bandegharaei, Production of Biochar from Melia Azedarach Seeds for Crystal Violet Dye Removal from Water: Combining of Hydrothermal Carbonization and Pyrolysis, Bioengineered, Vol. 14, 2023, pp. 290-306, https://doi.org/10.1080/21655979.2023.2236843.

[19] G. O. E. Sayed, Removal of Methylene Blue and Crystal Violet from Aqueous Solutions by Palm Kernel Fiber, Desalination, Vol. 272, 2011, pp. 225-232, https://doi.org/10.1016/j.desal.2011.01.025.

[20] S. Chakraborty, S. Chowdhury, P. D. Saha, Insight into Biosorption Equilibrium, Kinetics and Thermodynamics of Crystal Violet onto Ananas Comosus (Pineapple) Leaf Powder, Applied Water Science, Vol. 2, 2012, pp. 135-141, https://doi.org/10.1007/s13201-012-0030-9.

[21] A. S. A. Wasidi, I. S. A. Ibtisam, Effective Removal of Methylene Blue from Aqueous Solution Using Metal-Organic Framework; Modelling Analysis, Statistical Physics Treatment, and DFT Calculations, ChemistrySelect, Vol. 6, 2021, pp. 11431-11447, https://doi.org/10.1002/slct.202102330.

[22] A. K. Kushwaha, N. Gupta, M. C. Chattopadhyaya, Adsorption behavior of lead onto a New Class of Functionalized Silica Gel, Arabian Journal of Chemistry, Vol. 10, 2017, pp. 81-89, https://doi.org/10.1016/j.arabjc.2012.06.010.